

DOI: 10.1002/ ((please add manuscript number))

Article type: Full Paper

Title: Modulation of mechanical interactions by local piezoelectric effects

Cameron P. Brown^{1}, Jennifer L. Boyd¹, Antony J. Palmer¹, Mick Phillips², Charles-Andre Couture³, Maxime Rivard³, Philippa A. Hulley¹, Andrew J. Price¹, Andreas Ruediger³, Francois Légaré³, Andrew J. Carr*

Dr C.P. Brown, Dr J.L. Boyd, A.J. Palmer, Prof. P.A. Hulley, Prof. A.J. Price, Prof. A.J. Carr
Botnar Research Centre, NDORMS, University of Oxford, Old Road, Oxford OX3 7LD, UK.
E-mail: cameron.brown@ndorms.ox.ac.uk

Dr M. Phillips
Micron Oxford, Department of Biochemistry, University of Oxford, South Parks Road,
Oxford, OX1 3QU, UK

C-A. Couture, Dr M. Rivard, Prof. A. Ruediger, Prof. F. Légaré
INRS-EMT, 1650 Boulevard Lionel-Boulet, Varennes, Qc, J3X1S2, Canada.

Keywords: piezoelectricity, collagen, friction, biomimicry, mechanics

Piezoelectricity is a well-established property of biological materials, yet its functional role has remained unclear. Here, we demonstrate a mechanical effect of piezoelectric domains resulting from collagen fibril organisation, and describe its role in tissue function and application to material design. Using a combination of scanning probe and nonlinear optical microscopy, we observed a hierarchical structuring of piezoelectric domains in collagen-rich tissues, and explored their mechanical effects in silico. Local electrostatic attraction and repulsion due to shear piezoelectricity in these domains modulate fibril interactions from the tens of nanometre (single fibril interactions) to the tens of micron (fibre interactions) level, analogous to modulated friction effects. The manipulation of domain size and organisation thus provides a capacity to tune energy storage, dissipation, stiffness and damage resistance.

1. Introduction

Collagen is the most abundant protein in the human body and as one of the principal building blocks of tissues, plays a dominant role in the functioning of tendon, ligament, bone, cartilage, skin, heart and blood vessels. As such, its function is central to materials-based strategies for regenerative medicine, as well as providing a biomimetic target for high-performance, multifunctional fibre-based materials in applications outside of biomedicine. The defining feature of collagen is an elegant structural motif in which three parallel polypeptide strands coil with a one-residue stagger to form a right-handed triple helix, known as tropocollagen^[1] (**Figure 1**). Tropocollagen is unstable at body temperature,^[2] driving its formation into supertwisted, right-handed microfibrils with molecules packed in a quasi-hexagonal lattice.^[3] This leads to a spiral-like structure within the mature collagen fibril, with interdigitated microfibrils forming a networked, nanoscale rope.^[3, 4]

The complex hierarchical structure within a collagen fibril provides interesting mechanical^[5] and electrical^[6] properties, and the basis for interactions with other tissue components. This allows collagen to modulate tissue structure^[7] and therefore function. Through organisation and interactions on the nanometre to micrometre scales, collagen can work effectively in a wide variety of tissue configurations to provide exceptional mechanical performance, tuned to specialised applications.^[8, 9] The piezoelectric nature of collagen-rich tissues has been known for some time^[10] yet the role of collagen piezoelectricity in the body has remained elusive.^[11] Here, we report its role in modulating the mechanical functioning and interactions of collagen structures, and describe opportunities for translation to functional materials development for the wider biomaterials and engineering fields.

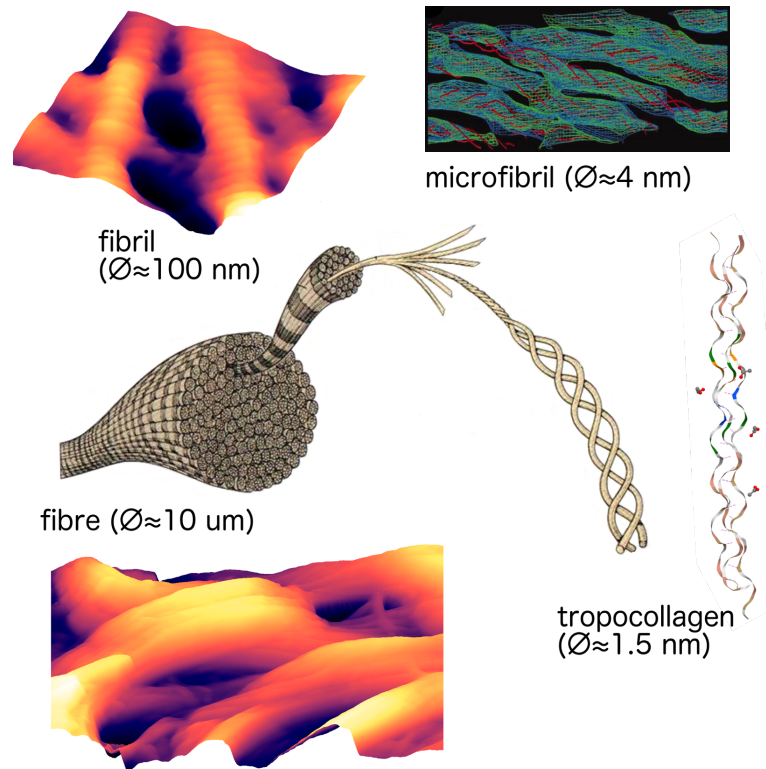


Figure 1. Collagen is hierarchically structured and organised from the nanometre scale of tropocollagen to the micrometre scale of the fibre, imparting properties and functionality in a range of tissues and environments. Idealised tropocollagen structure from the RCSB Protein Databank;^[12] electron density map showing microfibrils from;^[3] scanning probe images of fibrils and fibres captured by CPB and MP. Schematic of hierarchy reproduced from.^[13]

2. Results and Discussion

Using piezoresponse force microscopy (PFM) we observed distinct piezoelectric domains on the tens of nanometre to micron scale in human tendon (**Figure 2a**), and other tissues (**Figure S1**), resulting from the organisation of collagen fibrils. A constant piezoelectric property (d_{15} coefficient) was measured across each fibril and along its length, in agreement with previous results from isolated fibrils.^[14] The magnitude of the d_{15} coefficient of collagen was approximately 1 pm/V.^[14-16] Fibrils with the same sign of d_{15} , defined here as ‘polarity’, were grouped into ‘domains’ of adjacent fibrils. A dominant polarity was observed in any given region, broken by individual, or small groups of, oppositely polarised fibrils.

At a higher level of hierarchy (1 to 500 μm), similar patterns were observed optically using interferometric second harmonic generation imaging (iSHG, **Figure 2b**).^[17-19] This showed

the magnitude and sign of the average second order nonlinear optical susceptibility $\chi^{(2)}$ within the focal volume of the laser, which is equivalent to the piezoelectric tensor \mathbf{d} . Regions of predominantly positive and negative $\chi^{(2)}$, indicating predominant collagen fibril polarity, were maintained over distances of 5 to 50 μm perpendicular to the fibrils and hundreds of microns in the fibril direction.

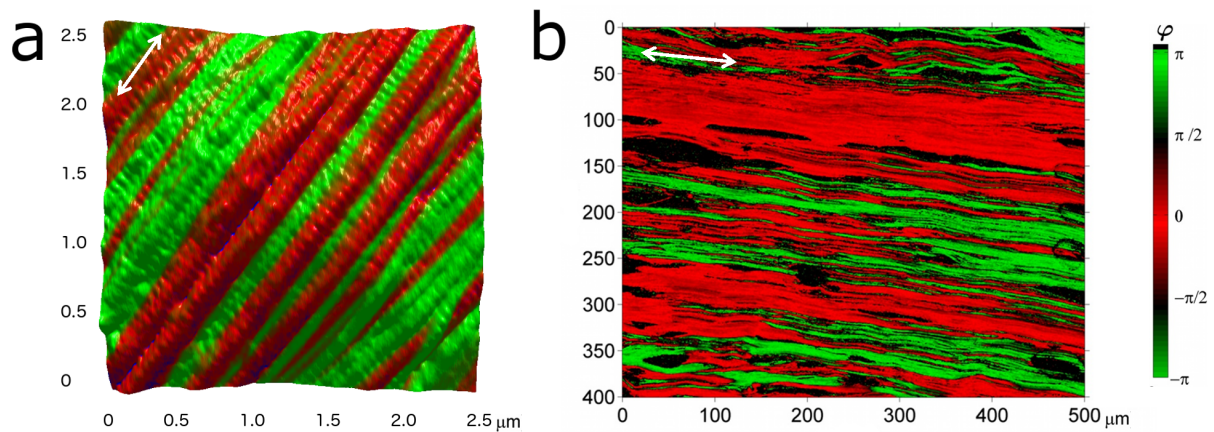


Figure 2. Piezoelectric domains in human hamstring tendon. (a) PFM image showing the distribution of piezoelectric properties at the fibril level. Both multi-fibril and single-fibril domains were observed, with most domains containing 3-6 fibrils. (b) iSHG showing the orientation of collagen polarity at a higher hierarchical level. Red and green indicate a phase ϕ of approximately 0 and π respectively, and therefore different signs of the \mathbf{d} and $\chi^{(2)}$ tensors in (a) and (b), with brightness indicating signal magnitude. White arrows indicate fibril direction.

To investigate the mechanical and electrical consequences of the observed piezoelectric domains, and opportunities for translation to functional materials, we developed finite element models of collagen fibril sliding. Under simple shear conditions replicating measured inter-fibril sliding on the order of 10-40° in tendon,^[20] a potential difference of 0.15 mV was calculated across the diameter of each fibril (**Figure 3**). Adjacent fibrils of similar polarity had the same sign of potential difference and therefore opposite charges accumulated at the interface (**Figure 3a,b**). These fibrils were electrostatically attracted and ‘stick’. Reversing the polarity of one of the fibrils reversed its potential difference, with like charges at the interface (**Figure 3c,d**), leading to electrostatic repulsion and slipping.

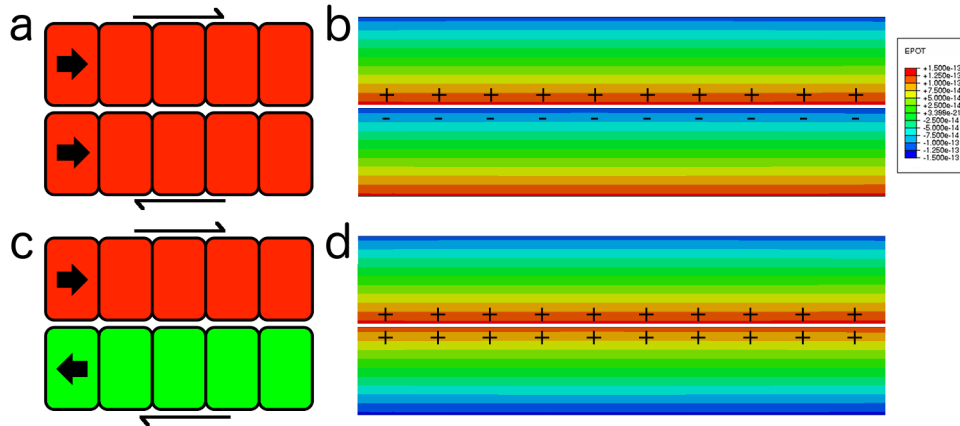


Figure 3. Simple model of piezoelectricity in two adjacent fibrils under shear for (a,b) the same polarity – i.e. within a domain, and (c,d) opposite polarities – i.e. at a domain boundary. Polarity is shown by colour and block arrows in (a) and (c). Colouring in (b) and (d) shows the distribution of electrical potential, with resultant charge accumulation at the fibril interface shown as ‘+’ or ‘-’. Attractive (+-) electrostatic forces were observed under shear between fibrils of the same polarity, and repulsive (either ++ or --) forces between fibrils of opposite polarity. Note that white lines have been overlaid at the fibril interfaces in (b) and (d) to mark the fibril boundaries.

A model of 20 interacting fibrils was developed to test these effects in the context of multiple fibril interfaces (**Figure 4, 5**). With a relative permittivity of 3 for wet collagen^[21] and an electrical potential of 0.15 mV from our 2-fibril simulation, Coulomb’s law gives an electrostatic force per unit area of approximately $1.8 \times 10^{-7} / r^2 \text{ Nm}^{-2}$ in water, where r is the distance between the charged surfaces. This effect was represented by manipulating the friction coefficient based on its linear relationship with the local normal force that is modulated by the attractive/repulsive forces. Increased effective friction at interfaces caused by attractive forces within piezoelectric domains locked the fibrils together, thus increasing storage of elastic energy within each domain prior to the onset of slip (**Figure 5c**). Fibrils stored 15 times more strain energy within domains than at the domain interface at the point of slipping, fitting observations of highly elastic behaviour within the larger fibre structures.^[22] When slipping did occur, the high friction within the domains increased the dissipation of energy (**Figure 5a**). At applied shear strains ≈ 1 for example, at which point all fibrils were slipping, the piezoelectric domains in the 20-fibril system increased the frictional dissipation

of energy by 30-50%, or 20-25% when normalised against external work. By modulating the domain size, or distribution of fibrils breaking domain continuity, the maximum shear could be tuned to minimise damage, while optimising the storage and dissipation of energy.

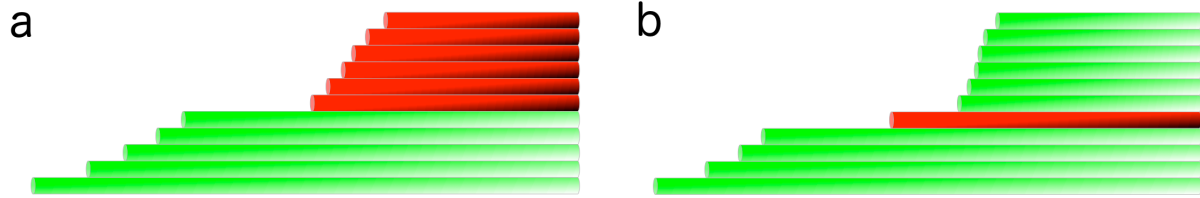


Figure 4: Deformation patterns of extracted regions of the 20-fibril models: (a) opposing domains, and (b) opposing fibrils, under shear. Red and green represent opposite polarity.

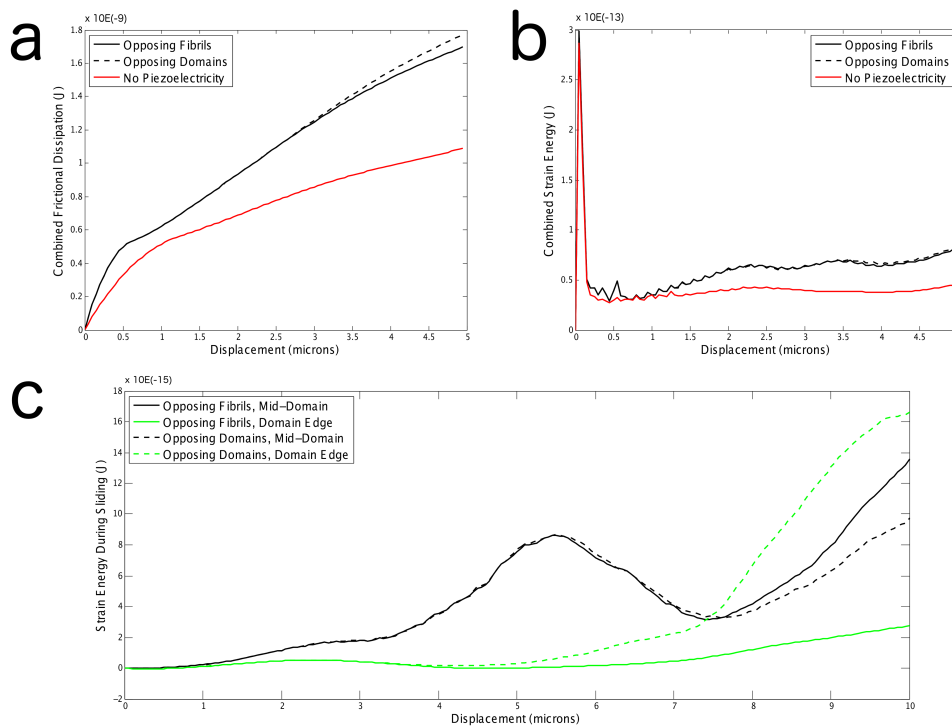


Figure 5. Frictional dissipation (a) and strain energy (b), calculated over the total region of the 20 interacting fibrils, were increased during sliding with the introduction of piezoelectric effects. Energy storage was markedly increased within domains, relative to the domain edge (c). The patterns of strain energy with deformation suggest a stick-slip action within domains, allowing mechanical performance to be maintained over large deformations.

The influence of piezoelectric domains on material toughness can be understood in the context of composite fibre models. Here, the higher local shear stress environment inside

domains is more likely to initiate fracture of individual fibrils,^[5] and capacity for energy storage must be balanced against fracture resistance. The increase in stress, and thus propensity to failure, limits domain size: domains of 3-6 fibrils in plane were typically observed in our samples. Microfracture within domains is preferred, however, due to the ‘sticking’ effect. Upon individual fibril fracture, fibril slipping will allow stress to be more effectively redistributed both across and along a domain than at an interface, protecting against the formation of a critical fracture cluster.^[23] The stick-slip mechanism observed within the domains (**Figure 5c**) further reconciles collagen fibril interactions to those within other high performance fibres such as spider silk.^[24] The piezoelectric modulation of load sharing and increase in effective strength distribution by domain formation will further suppress catastrophic cracking due to blocking effects.^[25]

2.1. Influence of piezoelectricity on biological material function

In the context of biological material function, the generation of attractive and repulsive forces responsible for the above-described effects depends on the level of fibril-fibril contact. Contact conditions are complicated by roughness (5-10 nm) due to banding, interference from non-collagenous proteins and the presence of low viscosity, dielectric interstitial fluid, including shielding from dissolved Na^+ and Cl^- . Local piezoelectric effects, generated through direct contact, are therefore stronger than regional effects, particularly with mixed domains at the tens to hundreds of micron scale. With large numbers of interaction sites, however, there is substantial capacity for the electrostatic interactions generated by shear to affect macroscopic material function.

In tendon and ligament for example, inter-fibril shear is a dominant loading mechanism,^[20] yet contact forces and local slipping distances are small.^[22] Interaction, however, sites are numerous. The hamstring tendon used in this study, semitendinosis, is $11.4 \pm 2.06 \text{ mm}^2$ in

cross sectional area^[26] with collagen fibrils of diameter 116.6 ± 79.26 nm and a filling fraction of 73.15 ± 15.8 .^[27] This gives approximately 1.1×10^9 fibrils per cross section. Fibrils in Achilles tendon, for comparison, are smaller in diameter, and with a fibril density of approximately 100 per μm^2 ^[28] and a cross-sectional area of $60\text{-}80$ mm^2 ,^[29] gives $6\text{-}8 \times 10^9$ fibrils per cross section.

The preferential grouping of fibrils into domains of similar polarity may provide insight in to the probabilistic dynamics of fibril interactions during development, remodelling and disease. Here, the short distance (few nm) over which the electrostatic force will act, particularly in a shielding physiological fluid environment, requires direct fibril-fibril contact to preferentially form domains from a matrix of randomly polarised fibrils. The similarity in domain size and organisation between different tissues (**Figure S1**; see also ^[14, 30]) therefore suggests that cohesive strength is consistent with the prevailing mechanical environment in developing and healthy mature tissue, restricting of fibril motility to a similar degree. The repulsive regime at the domain interface may further define and distribute microchannels for fluid movement, which in turn plays a central role in tissue viscoelasticity, damage resistance, mechanotransduction and nutrient transport.^[31] The inverse effect of local shear deformation in an electric field may explain the effect of cyclic electrical stimulation on tissue healing and observed effects of field polarity^[32] by triggering shear micromotion and fluid movement.

In diseased tissue, however, in which the cohesion of the collagen network is disrupted,^[33, 34] the increased fibril motility is apparent from observations of large bundles of fibrils with the same piezoelectric polarity, causing stress concentrations that drive disease progression.^[18, 35]

In early-stage osteoarthritic cartilage for example, bundles sizes of 30-50 fibrils are observed.^[18] Similar increases in domain size are observed in diseased tendon (50-60 fibrils based on forwards:backwards ratio ≈ 13.5 ,^[18] **Figure S2**).

Given that energetic effects rather than entropic contributions govern the elastic and fracture properties of collagen fibrils and fibres,^[36] the energetic contributions from piezoelectricity-modulated interactions extends mechanical representations of collagen^[e.g. 5, 36, 37] to the mesoscale, enabling further exploration of hierarchical toughening effects. Updating the physics of collagen behaviour under load also resolves outstanding questions regarding the mechanics of collagen-based tissues. Of particular importance to tendon and ligament modelling is the implication for load sharing.^[20] Recent experiments have shown that proteoglycans, the proteins traditionally implicated in stress sharing between fibrils,^[38] assist rather than restrict sliding.^[39] The structural basis for explaining microscale tissue mechanics^[20] is therefore problematic. The mechanics of collagen network entanglement, for example in cartilage,^[34] and its role in tissue function, are similarly unresolved.

Piezoelectricity, however, may advance our understanding of tissue function, providing a mechanism through electrostatic attraction or repulsion for the local modulation of shear lag.

At the level of fibre interactions (micrometre to hundreds of micrometres), the switching of dominant polarities, the resultant increase in the probability of electrostatic repulsion between fibres and therefore probability of slipping, fits with observations of larger inter-fibre deformations relative to intra-fibre deformations.^[22] Similar regions of dominant polarity have been observed in cartilage, with highly aligned fibrils observed at the region interfaces^[19] further supporting the increased probability of sliding. Measured piezoelectric behaviour at the tissue level in tendon^[10] and cartilage^[40] further indicate polarisation dominance higher hierarchical levels than studied here. As stated above, fluid, non-collagenous proteins and the mixture of domains limit the strength of piezoelectric effects at this hierarchical level. Rather than simple attraction or repulsion of the bulk regions, piezoelectric interactions are therefore likely to encourage formation and interdigitation of bundles, similar to the bond-modulated interaction of twisted microfibrils at the nanometre scale.^[3, 5]

2.2. Applications of piezoelectric domain organisation in synthetic materials

The mechanism of tuning the performance of collagen constructs provides new opportunities for applying synthetic piezoelectric materials. Control over adhesion and friction is critical in any mechanical system,^[41] and is of particular interest at smaller size scales due to large surface-to-volume ratios.^[42] Expanding current piezoelectric energy harvesting and sensing applications,^[43] the interactions between piezoelectric materials may thus be used as passive components for example to control tribology in nano- or microelectromechanical systems (NEMS/MEMS) and microfluidics, to tune mechanical performance in fibre-based or layered systems, or to predispose mesoscopic self assembly processes in dynamic mechanical environments. By controlling the magnitudes and signs shear piezoelectric coefficients in adjacent components or layers, their interactions can be controlled. The simplest application of this may be to improve lubrication between surfaces by using domains of opposite polarity at the contact surfaces. By generating repulsive forces at the surfaces, solid-solid contact will be minimised, reducing friction in the low-speed boundary lubrication regime and promoting the onset of hydrodynamic lubrication regimes by encouraging surface separation.

More advanced, active applications of piezoelectric domain organisation may be in wearable or implantable biomedical systems,^[44] allowing control over directionality and spatial distributions of active mechanical effects, to target specific movements with sensors, or to match the mechanical properties of a device to that of the host tissue. Finally, combining piezoelectric materials with other tribological strategies (such as those involving 2-D materials,^[45] nanocomposites,^[46] or charged polymer brushes^[47]) may extend performance. Piezoelectric materials can also be modified, for example, by laser texturing,^[48] to further improve tribology, generating higher shear strains at contact points, thus increasing local electrostatic repulsion.

3. Conclusion

Collagen fibrils have a d_{15} (shear) coefficient of approximately 1 pm/V, and organise into hierarchical domains of piezoelectric polarity. Local electrostatic attraction and repulsion due to shear piezoelectricity modulates fibril interactions from the tens of nanometre to the tens of micron level. The manipulation of domain size and organisation allows control over fibril interactions and therefore a capacity to tune energy storage, dissipation, stiffness and damage resistance. In addition to understanding natural material function, this mechanism provides a basis to introduce passive piezoelectric components or surfaces to modulate interactions in synthetic systems.

4. Experimental Section

Experimental Method

Tendon was chosen as a material in which to explore piezoelectric effects due to its high content of collagen I,^[27] the most abundant collagen in humans, its highly ordered ultrastructure, and the sliding behaviour across hierarchical levels^[5, 22] with potential to trigger shear piezoelectric behaviour of collagen. Healthy human hamstring tendon was taken from leftover tissue used for anterior cruciate ligament reconstruction with informed consent. For scanning probe microscopy measurements, samples were snap frozen, cryosectioned at 5 μm and mounted on glass coverslips. Cryosectioned articular cartilage and polished ivory cross-sections were measured for comparison. For interferometric second harmonic generation (ISHG) measurements, samples were cryosectioned at 10 μm , mounted on glass slides and coverslipped.

Scanning probe microscopy was performed on a Cypher AFM and MFP-3D AFM (Asylum Research, High Wycombe, UK). Measurements were performed using intermittent-contact

mode^[49] and lateral piezoresponse force microscopy (PFM).^[30, 50] The experimental setup for ISHG measurements is described in Rivard et al.^[17] Building on the work of refs^[51] this examines the orientation of collagen within the laser focal volume. In summary, the laser source was a ~15 ps pulse duration 1064 nm 80 MHz oscillator (Vanguard, Spectra Physics, Santa Clara, USA). The beam was loosely focussed near the interface of a 350 μm thick polished Y-cut quartz crystal, generating a low power SHG reference beam, which interfered with the SHG from the sample. The relative phase of the reference beam was controlled using an angled glass plate, and a polariser used to maximise the interferometric contrast detected by the photomultiplier tube.

Computational Method

Finite element models were developed to explore the effects of the observed piezoelectric domains in the context of tissue behaviour. We did not attempt to replicate the extensive work by Buehler, Fratzl and colleagues^[5, 8, 52] on the mechanical response of collagen itself, instead focussing on the use of collagen interactions to modulate mechanical performance and damage resistance. Limited information is available on shear stress in tendon. Based on axial loading of rat tail fascicles, inter-fibril shear stress on the order of 1 kPa have been calculated from numerical models.^[20] Shear deformations between fibrils, however, have been measured directly, with inter-fibril sliding on the order of 10-40 degrees.^[20] The reproduction of this range of inter-fibril sliding has been the focus of our models. To our knowledge, neither shear stress nor strain has been measured in the fibrils themselves.

Modelling was undertaken in two stages. First, a model of two interacting fibrils was developed to investigate the local effects of the piezoelectric property of collagen. A 2-D implicit model was developed in Abaqus (v 6.11), using piezoelectric elements (CPE8RE). Collagen fibrils were represented with diameter 100 nm, based on our AFM results, with fibril

length 1 μm . The collagen material was modelled as linear elastic isotropic (elastic modulus 200 MPa,^[53] Poisson's ratio 0.35), with the d_{15} coefficient of the piezoelectric tensor 1 pm/V.^[14, 15] The two fibrils of interest were loaded by adjacent external fibrils to simulate a continuous boundary condition, first in compression (125 μN) to achieve firm contact, and then in shear (500 μN) to invoke piezoelectricity. The resulting electrical potential across each fibril was calculated for both similar and opposite polarisations. Fibrils were not allowed to fracture.

Using the local electrostatic attraction or repulsion caused by the piezoelectric response as an input, a second set of models was developed to investigate the effect of piezoelectric domains in the context of multiple fibril interfaces. This attractive or repulsive force was represented by modulating the coefficient of friction, utilising its linear relationship with the normal force in determining resistance to sliding ($F_f = \mu F_N$ where μ is the coefficient of friction between fibrils and F_N is the normal force caused by the collagen piezoelectric response). This set of models used a 2-D explicit solution with 20 fibrils of the same material properties as the two-fibril model, using CPS6M elements. An 'opposing fibrils model' incorporated single fibrils were within a large domain of opposite polarity. An 'opposing sections model' incorporated three sections of fibrils, with adjacent sections of opposite polarity. In each case the outer fibrils were 50 μm long, and the inner 18 fibrils 20 μm long. Again, fibrils were uniformly compressed to achieve firm contact at each interface, and the top and bottom fibrils axially translated to induce shear. Mesh sizes and solution time increments were identical between models. The strain energy, external work, and frictional dissipation calculated by the models were stored and compared.

Supporting Information

Supporting Information is available from the Wiley Online Library or from the author.

Acknowledgements

We gratefully acknowledge support from Arthritis Research UK (grant 20299 and Oxford EOTC), Marie Curie IRSES *skelGEN*, the Oxford Musculoskeletal Biobank and the Oxford NIHR BRU.

Received: ((will be filled in by the editorial staff))

Revised: ((will be filled in by the editorial staff))

Published online: ((will be filled in by the editorial staff))

References

- [1] M. D. Shoulders, R. T. Raines, *Annual Review of Biochemistry* 2009, 78, 929.
- [2] E. Leikina, M. V. Merts, N. Kuznetsova, S. Leikin, *PNAS* 2002, 99, 1314.
- [3] J. P. R. O. Orgel, T. C. Irving, A. Miller, T. J. Wess, *PNAS* 2006, 103, 9001.
- [4] L. Bozec, G. van der Heijden, M. Horton, *Biophys. J.* 2007, 92, 70.
- [5] A. Gautieri, S. Vesentini, A. Redaelli, M. J. Buehler, *Nano Lett* 2011, 11, 757.
- [6] J. C. Anderson, C. Eriksson, *Nature* 1968, 218, 166; M. Minary-Jolandan, M.-F. Yu, *ACS Nano* 2009, 3, 1859.
- [7] B. Trappmann, J. E. Gautrot, J. T. Connelly, D. G. T. Strange, Y. Li, M. L. Oyen, M. A. Cohen Stuart, H. Boehm, B. Li, V. Vogel, J. P. Spatz, F. M. Watt, W. T. S. Huck, *Nat Mater* 2012, 11, 642; Y. Wang, T. Azaïs, M. Robin, A. Vallée, C. Catania, P. Legriel, G. Pehau-Arnaudet, F. Babonneau, M.-M. Giraud-Guille, N. Nassif, *Nat Mater* 2012, 11, 724.
- [8] A. K. Nair, A. Gautieri, S.-W. Chang, M. J. Buehler, *Nat Commun* 2013, 4, 1724.
- [9] E. A. Zimmermann, B. Gludovatz, E. Schaible, N. K. N. Dave, W. Yang, M. A. Meyers, R. O. Ritchie, *Nat Commun* 2013, 4; C. P. Brown, *Nature Reviews Rheumatology* 2013, 9, 614.
- [10] E. Fukada, I. Yasuda, *Jpn. J. Appl. Phys.* 1964, 3, 117.
- [11] A. Gruverman, B. Rodriguez, S. Kalinin, in *Scanning Probe Microscopy*, (Eds: S. Kalinin, A. Gruverman), Springer New York, 2007, 615.
- [12] R. Z. Kramer, J. Bella, P. Mayville, B. Brodsky, H. M. Berman, *Nature Structural Biology* 1999, 6, 454.
- [13] N. A. Campbell, *Biology*, Benjamin-Cummings Pub Co, Menlo Park, California 1995.
- [14] C. Harnagea, M. Vallières, C. P. Pfeffer, D. Wu, B. R. Olsen, A. Pignolet, F. Légaré, A. Gruverman, *Biophys. J.* 2010, 98, 3070.
- [15] K. S.V., B. J. Rodriguez, S. Jess, T. Thundat, A. Gruverman, *Applied Physics Letters* 2005, 87, 053901.
- [16] M.-J. Majid, Y. Min-Feng, *Nanotechnology* 2009, 20, 085706.
- [17] M. Rivard, K. Popov, C.-A. Couture, M. Laliberté, A. Bertrand-Grenier, F. Martin, H. Pépin, C. P. Pfeffer, C. Brown, L. Ramunno, F. Légaré, *Journal of Biophotonics* 2013, 1, 233.
- [18] C. P. Brown, M.-A. Houle, K. Popov, M. Nicklaus, C.-A. Couture, M. Laliberté, T. Brabec, A. Ruediger, A. J. Carr, A. J. Price, H. S. Gill, L. Ramunno, F. Légaré, *Biomed Opt Exp* 2014, 5, 233.
- [19] C.-A. Couture, S. Bancelin, J. Van der Kolk, K. Popov, M. Rivard, K. Legare, G. Martel, H. Richard, C. P. Brown, S. Laverty, L. Ramunno, F. Legare, *Biophys. J.* 2015, 109, 2501.
- [20] S. E. Szczesny, D. M. Elliott, *Acta Biomaterialia* 2014, 10, 2582.
- [21] E. Marzec, K. Pietrucha, *Biophysical Chemistry* 2008, 132, 89.

- [22] H. R. C. Screen, D. L. Bader, D. A. Lee, J. C. Shelton, *Strain* 2004, 40, 157.
- [23] S. Pimenta, S. T. Pinho, *Journal of the Mechanics and Physics of Solids* 2013, 61, 1337.
- [24] C. P. Brown, C. Harnagea, H. S. Gill, A. J. Price, E. Traversa, S. Licoccia, F. Rosei, *ACS Nano* 2012, 6, 1961.
- [25] S. Mahesh, S. L. Phoenix, I. Beyerlein, *International Journal of Fracture* 2002, 115, 41.
- [26] W. Pichler, N. P. Tesch, G. Schwantzer, G. Fronhöfer, C. Boldin, L. Hausleitner, W. Grechenig, *A CADAVER STUDY* 2008, 90-B, 516.
- [27] P. T. Hadjicostas, P. N. Soucacos, H. H. Paessler, N. Koleganova, I. Berger, *Arthroscopy: The Journal of Arthroscopic & Related Surgery* 2007, 23, 751.
- [28] S. P. Magnusson, K. Qvortrup, J. O. Larsen, S. Rosager, P. Hanson, P. Aagaard, M. Krogsgaard, M. Kjaer, *Matrix Biology* 2002, 21, 369.
- [29] W. A. Schmidt, H. Schmidt, B. Schicke, E. Gromnica-Ihle, *Annals of the Rheumatic Diseases* 2004, 63, 988.
- [30] D. Denning, S. Alilat, S. Habelitz, A. Fertala, B. J. Rodriguez, *J. Struct. Biol.* 2012, 180, 409.
- [31] A. J. Grodzinsky, M. E. Levenston, M. Jin, E. H. Frank, *Annual Review of Biomedical Engineering* 2000, 2, 691; M. Lavagnino, S. Arnoczky, E. Kepich, O. Caballero, R. Haut, *Biomech Model Mechanobiol* 2008, 7, 405; H. Ahmadzadeh, B. R. Freedman, B. K. Connizzo, L. J. Soslowsky, V. B. Shenoy, *Acta Biomaterialia* 2015, 22, 83.
- [32] A. F. Ahmed, S. S. A. Elgayed, I. M. Ibrahim, *Journal of Advanced Research* 2012, 3, 109; K. C. Balakatounis, A. G. Angoules, *Eplasty* 2008, 8, e28.
- [33] N. D. Broom, H. Silyn-Roberts, *Arthritis and Rheumatism* 1990, 33, 1512.
- [34] N. D. Broom, M.-H. Chen, A. Hardy, *Journal of Anatomy* 2001, 199, 683.
- [35] C. P. Brown, M.-A. Houle, M. Chen, A. J. Price, F. Légaré, H. S. Gill, *J. Mech. Behav. Biomed. Mat.* 2012, 57, 547.
- [36] M. J. Buehler, *PNAS* 2006, 103, 12285.
- [37] M. J. Buehler, *J Mech Behav Biomed Mater* 2008, 1, 59.
- [38] A. Redaelli, S. Vesentini, M. Soncini, P. Vena, S. Mantero, F. M. Montevercchi, *Journal of Biomechanics* 2003, 36, 1555.
- [39] S. Rigozzi, R. Müller, A. Stemmer, J. G. Snedeker, *Journal of Biomechanics* 2013, 46, 813.
- [40] C. A. L. Bassett, R. J. Pawluk, *Science* 1972, 178, 982.
- [41] A. Vanossi, N. Manini, M. Urbakh, S. Zapperi, E. Tosatti, *Reviews of Modern Physics* 2013, 85, 529.
- [42] B. Bhushan, J. N. Israelachvili, U. Landman, *Nature* 1995, 374, 607; E. Koren, E. Lörtscher, C. Rawlings, A. W. Knoll, U. Duerig, *Science* 2015, 348, 679.
- [43] W. Tong, Y. Zhang, Q. Zhang, X. Luan, F. Lv, L. Liu, Q. An, *Advanced Functional Materials* 2015, n/a; R. Hinchet, S. Lee, G. Ardila, L. Montès, M. Mouis, Z. L. Wang, *Advanced Functional Materials* 2014, 24, 971; J.-H. Lee, H.-J. Yoon, T. Y. Kim, M. K. Gupta, J. H. Lee, W. Seung, H. Ryu, S.-W. Kim, *Advanced Functional Materials* 2015, 25, 3203.
- [44] W. Zeng, L. Shu, Q. Li, S. Chen, F. Wang, X.-M. Tao, *Advanced Materials* 2014, 26, 5310; G.-T. Hwang, M. Byun, C. K. Jeong, K. J. Lee, *Advanced Healthcare Materials* 2015, 4, 646.
- [45] D. Berman, S. A. Deshmukh, S. K. R. S. Sankaranarayanan, A. Erdemir, A. V. Sumant, *Advanced Functional Materials* 2014, 24, 6640.
- [46] L. Rapoport, O. Nepomnyashchy, A. Verdyan, R. Popovitz-Biro, Y. Volovik, B. Ittah, R. Tenne, *Advanced Engineering Materials* 2004, 6, 44.
- [47] U. Raviv, S. Giasson, N. Kampf, J.-F. Gohy, R. Jerome, J. Klein, *Nature* 2003, 425, 163.
- [48] I. Etsion, *Tribology Letters* 2004, 17, 733.

- 1 [49] Q. Zhong, D. Inniss, K. Kjoller, V. B. Elings, Surface Science Letters 1993, 290, L688.
2 [50] L. M. Eng, H.-J. Güntherodt, G. A. Schneider, U. Köpke, J. Muñoz Saldaña, Applied
3 Physics Letters 1999, 74, 233; L. M. Eng, H. J. Guntherodt, G. Rosenman, A. Skliar, M. Oron,
4 M. Katz, D. Eger, Journal of Applied Physics 1998, 83, 5973.
5 [51] I. Freund, M. Deutsch, A. Sprecher, Biophys. J. 1986, 50, 693; D. A. D. Parry, A. S.
6 Craig, Biopolymers 1977, 16, 1015.
7 [52] A. Gautieri, M. I. Pate, S. Vesentini, A. Redaelli, M. J. Buehler, Journal of
8 Biomechanics 2012, 45, 2079; P. Fratzl, *Collagen: Structure and Mechanics*, Springer, New
9 York 2008.
10 [53] J. A. J. van der Rijt, K. O. van der Werf, M. L. Bennink, P. J. Dijkstra, J. Feijen,
11 Macromol. Biosci. 2006, 6, 697.
12

Table of contents

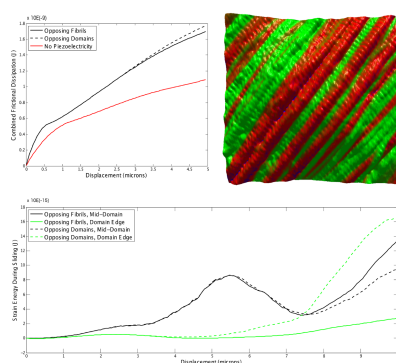
Domains of piezoelectricity passively modulate interactions in mechanical systems.

Mechanical analysis of piezoelectricity and its manifestation in collagen fibril interactions reveals that electrostatic attraction within domains, and repulsion at domain boundaries mediates mesoscale mechanical properties. This mechanism can be applied to functionalise synthetic systems by the introduction of passive piezoelectric materials to tune mechanical performance, damage resistance or tribology.

Piezoelectricity, friction, collagen, biomimicry, mechanics

Cameron P. Brown^{1*}, Jennifer L. Boyd¹, Antony J. Palmer¹, Mick Phillips², Charles-Andre Couture³, Maxime Rivard³, Philippa A. Hulley¹, Andrew J. Price¹, Andreas Ruediger³, Francois Légaré³, Andrew J. Carr

Modulation of mechanical interactions by local piezoelectric effects



Copyright WILEY-VCH Verlag GmbH & Co. KGaA, 69469 Weinheim, Germany, 2013.

Supporting Information

Modulation of mechanical interactions by local piezoelectric effects

Cameron P. Brown^{1*}, Jennifer L. Boyd¹, Antony J. Palmer¹, Mick Phillips², Charles-Andre Couture³, Maxime Rivard³, Philippa A. Hulley¹, Andrew J. Price¹, Andreas Ruediger³, Francois Légaré³, Andrew J. Carr

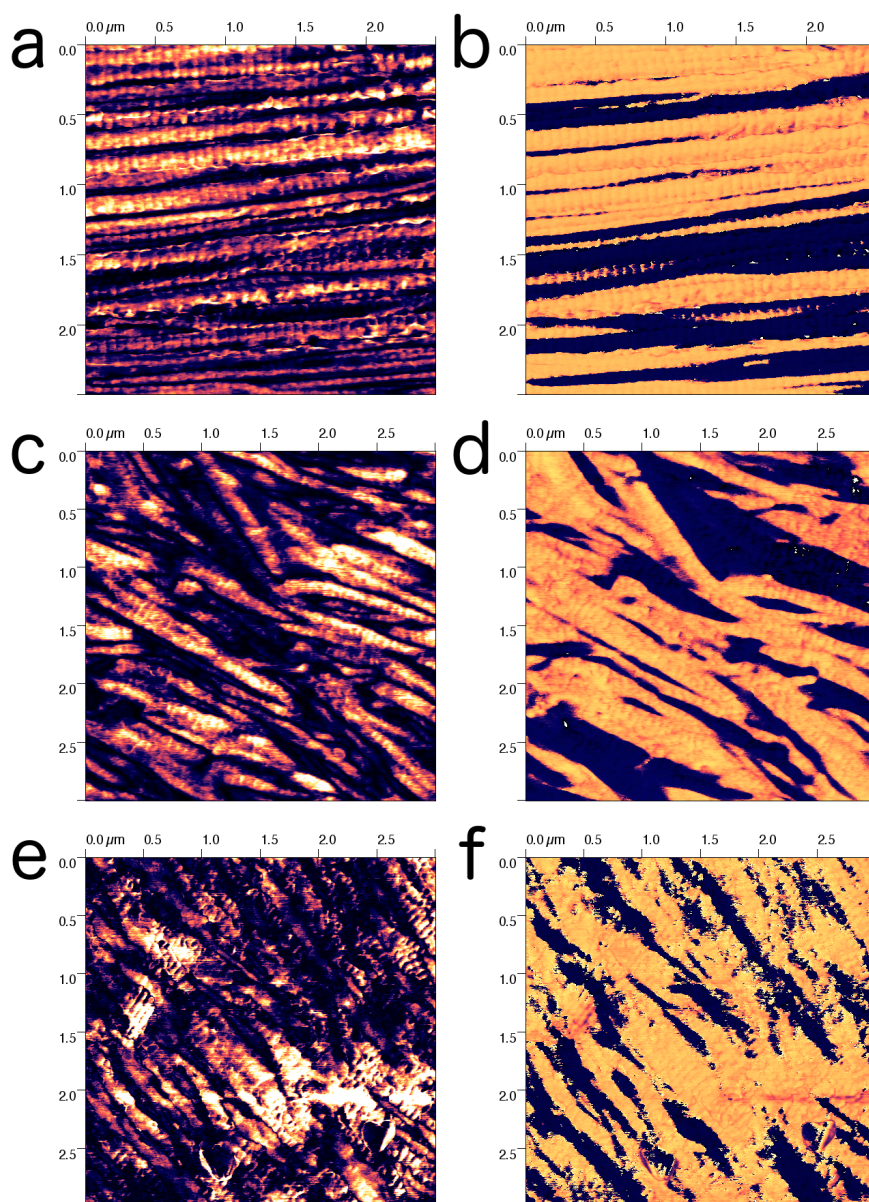


Figure S1. PFM images show the similar organisation of collagen polarity in different tissues/materials, despite their very different mechanical environments. A dominant polarity is observed in each case, with fibrils of the same polarity bundled together in small groups. (a,b) show amplitude of and phase, respectively, of piezoresponse of collagen in tendon, (c,d) in articular cartilage, and (e,f) in ivory. All images 3×3 μm.

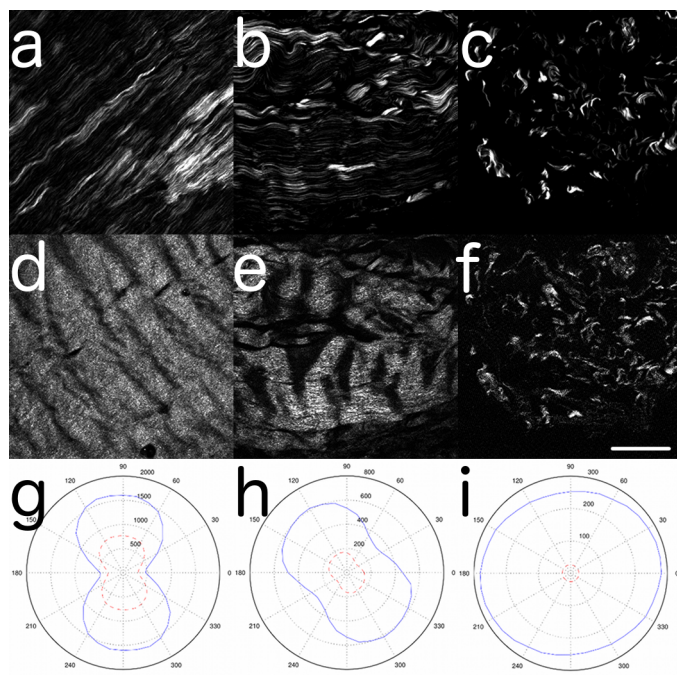


Figure S2. Forward SHG images (a-c), backward SHG images (d-f) and polarisation plots (g-i) of normal, early-stage diseased, and late-stage diseased tendon, respectively. Solid blue curves show the forwards signal, dashed red lines show the backwards signal. The forwards:backwards SHG ratio provides information on the bundling of fibres with the same polarity, with larger bundles giving higher ratios. Scale bar 50 μm .